Core level excitations—A fingerprint of structural and electronic properties of epitaxial silicene

R. Friedlein, A. Fleurence, K. Aoyagi, M. P. de Jong, H. Van Bui, F. B. Wiggers, S. Yoshimoto, T. Koitaya, S. Shimizu, H. Noritake, K. Mukai, J. Yoshinobu, and Y. Yamada-Takamura

Citation: The Journal of Chemical Physics **140**, 184704 (2014); doi: 10.1063/1.4875075
View online: http://dx.doi.org/10.1063/1.4875075
View Table of Contents: http://scitation.aip.org/content/aip/journal/jcp/140/18?ver=pdfcov
Published by the AIP Publishing

Core level excitations—A fingerprint of structural and electronic properties of epitaxial silicene

R. Friedlein,[1,a)] A. Fleurence,[1] K. Aoyagi,[1] M. P. de Jong,[2] H. Van Bui,[2] F. B. Wiggers,[2] S. Yoshimoto,[3] T. Koitaya,[3] S. Shimizu,[3] H. Noritake,[3] K. Mukai,[3] J. Yoshinobu,[3] and Y. Yamada-Takamura[1]

[1]*School of Materials Science, Japan Advanced Institute of Science and Technology (JAIST), 1-1, Asahidai, Nomi, Ishikawa 923-1292, Japan*
[2]*MESA+ Institute for Nanotechnology, University of Twente, 7500 AE Enschede, The Netherlands*
[3]*The Institute for Solid State Physics, The University of Tokyo, 5-1-5 Kashiwanoha, Kashiwa, Chiba 277-8581, Japan*

(Received 6 February 2014; accepted 24 April 2014; published online 12 May 2014)

From the analysis of high-resolution Si 2*p* photoelectron and near-edge x-ray absorption fine structure (NEXAFS) spectra, we show that core level excitations of epitaxial silicene on $ZrB_2(0001)$ thin films are characteristically different from those of sp^3-hybridized silicon. In particular, it is revealed that the lower Si 2*p* binding energies and the low onset in the NEXAFS spectra as well as the occurrence of satellite features in the core level spectra are attributed to the screening by low-energy valence electrons and interband transitions between π bands, respectively. The analysis of observed Si 2*p* intensities related to chemically distinct Si atoms indicates the presence of at least one previously unidentified component. The presence of this component suggests that the observation of stress-related stripe domains in scanning tunnelling microscopy images is intrinsically linked to the relaxation of Si atoms away from energetically unfavourable positions. © *2014 AIP Publishing LLC*. [http://dx.doi.org/10.1063/1.4875075]

I. INTRODUCTION

Silicene, the silicon analogue of graphene, is predicted to feature Dirac fermions at the Fermi level just like its carbon counterpart[1,2] offering a wealth of physical phenomena as well as bright perspectives for electronic applications. Spin-orbit coupling in silicene is predicted to be much larger than in graphene such that a large quantum spin Hall effect,[3,4] a topological phase transition,[5] and perfect spin filtering[6] could be realized. While the synthesis of free-standing silicene remains a major challenge, the preparation of two-dimensional, epitaxial Si honeycomb structures on metallic substrates, such as Ag(111),[7–9] $ZrB_2(0001)$,[10] and Ir(111)[11] allows a comprehensive characterization of structural, electronic, and chemical properties of the layers that could lead to a verification of properties unique to silicene.

It already became quite clear that both the structural and electronic properties of epitaxial silicene phases are substantially different from those of the yet hypothetical free-standing form.[7,8,10] For instance, the lack of Dirac fermions in silicene on Ag(111) has been reported recently.[12] Epitaxial silicene on the $ZrB_2(0001)$ surface has been shown to exhibit an atomistic buckling related to the $(\sqrt{3} \times \sqrt{3})$ reconstruction of the honeycomb lattice.[10] The reconstruction leads to the back-folding of electronic states into the reduced Brillouin zone and to the opening of a gap.[10] While some states in the vicinity of the Fermi level (E_F) visible in angle-resolved photoelectron (ARPES) spectra have been assigned to π bands,[10,13] details regarding the strength of hybridization with substrate electronic states and the resulting type of buckling are still subject of debate.[14]

In the present report, high-resolution Si 2*p* x-ray photoelectron (XPS) and near-edge x-ray absorption fine structure (NEXAFS) spectra of epitaxial silicene on the $ZrB_2(0001)$ thin film surface are discussed. It is well established that such core level spectra are very sensitive to the chemical environment and the bonding configuration in the vicinity of the Si atom where the excitation occurs.[15–18] Using these powerful spectroscopic techniques, we provide further insightful information on how atomic-scale buckling and the presence of π electrons determine core level excitations in epitaxial silicene.

II. EXPERIMENTAL

The Si 2*p* photoelectron spectra have been obtained using the SES-200 hemispherical analyzer at the end-station of the undulator beam line 13A at the Photon Factory synchrotron radiation facility, located at the High Energy Accelerator Research Organization (KEK), Tsukuba, Japan. The energy resolution was better than 50, 70, and 100 meV, for photon energies of $h\nu = 130$, 340, and 700 eV, respectively, as determined from the broadening of E_F measured at tantalum clamps nearby. Due to the fixed position of the analyzer at this end-station, in the normal-emission geometry employed in the measurements of the Si 2*p* core levels, the electric field vector of the light is at an angle of 25° with respect to the normal of the sample. The intensities have been normalized to the photon flux as measured with a gold grid mounted in the beam line.

a)Author to whom correspondence should be addressed. Electronic mail: friedl@jaist.ac.jp

NEXAFS spectra at the Si 2*p* threshold have been obtained using a custom-built microchannel plate (MCP) detector at beamline D1011 of the MAX-Lab synchrotron radiation facility in Lund, Sweden. Electrons have been collected in the partial yield mode with the suppression for kinetic energies below 30 eV. The photon-energy dependent intensity profile of the light used for the normalization of the spectra has been measured using a clean Ge sample. The absolute values of the photon energies have been calibrated using second-order light.

Oxide-free silicene samples have been prepared as described previously.[10,19] Briefly, in our experiments, silicene forms *in situ* and spontaneously through surface segregation on metallic single-crystalline zirconium diboride thin films on Si(111) wafers (P-doped, 3–5 Ωcm) after removing oxides by annealing of the samples at about 780 °C under ultra-high vacuum conditions (i.e., pressure below 3×10^{-9} mbar). During the measurements, samples were held at room temperature. The (2×2) reconstruction of the annealed $ZrB_2(0001)$ surface has been verified by low-energy electron diffraction.

III. RESULTS AND DISCUSSION

A. Si 2p core levels

Fig. 1(a) shows the normal-emission Si 2*p* spectrum obtained for $h\nu = 130$ eV, which resembles the one reported previously.[10] Due to the higher energy resolution, however, for both the $2p_{1/2}$ and $2p_{3/2}$ lines, two peaks can be recognized to be well separated from each other. Following the subtraction of the Shirley background, three components labelled α, β, and γ related to the A, B, and C atomic positions of the Si atoms within the $(\sqrt{3} \times \sqrt{3})$ unit cell of epitaxial silicene, shown in Fig. 1(b), are again identified by the peak fitting procedure using asymmetric Pseudo-Voigt functions described in detail previously.[10] Here it is important to remark that this initial assumption of three components is based on the structure model outlined recently for the honeycomb lattice within stripe domains visible in scanning tunnelling microscopy (STM) images.[10] As discussed in detail in Sec. III C, it is actually one of the goals of the present evaluation to show that this initial assumption does not hold and that at least one additional component is not accounted for.

For the peak fitting procedure using the initial assumption, for all of the three components labelled α, β, and γ, the same branching ratio of 2:1, and the same spin-orbit splitting of 600 meV have been employed. The same asymmetry parameters as well as Gaussian and Lorentzian widths have been used for the $2p_{1/2}$ and $2p_{3/2}$ lines. Note that the decision to keep these parameters fixed for both spin-orbit split lines has been taken in order to reduce the parameter set in the fitting procedure. Given the quite similar nature of the photoelectron transitions for the two lines, it might be reasonable to assume that vibrational progressions for the $2p_{1/2}$ and $2p_{3/2}$ transitions between the initial and final state potential surfaces, life times related to the photoelectron emission processes[20] as well as satellite features related to electron-hole pair excitation (or low-energy shake-up) and photoelectron energy loss processes effects might be quite similar to each other for the two lines.

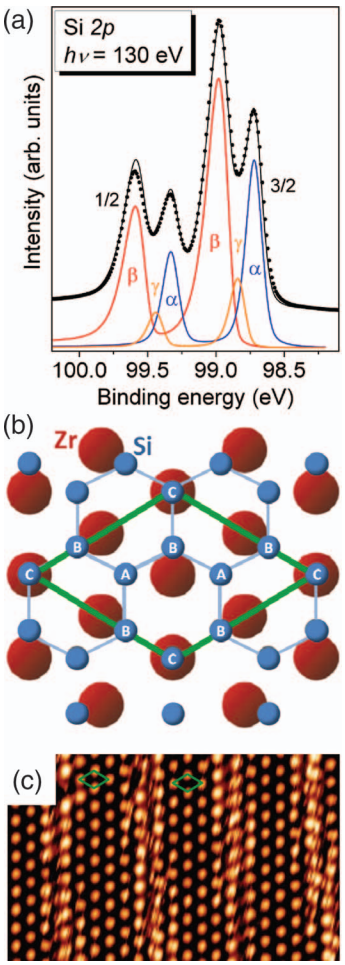

FIG. 1. (a) Surface-sensitive Si 2*p* photoelectron spectrum of silicene on a thin $ZrB_2(0001)$ film recorded at normal emission, using a photon energy of $h\nu = 130$ eV (●). Chemical states α, β, and γ are identified by a peak fitting procedure and relate to the three distinct atomic sites within the $(\sqrt{3} \times \sqrt{3})$-reconstructed and buckled honeycomb lattice. The full line (—) is the sum of the three components. (b) In-plane structure model of silicene on $ZrB_2(0001)$ within the center of stripe domains. The A, B, and C Si atoms are indicated together with the diamond-shaped unit cell of the (2×2)-reconstructed diboride surface. (c) STM image of silicene on the $ZrB_2(0001)$ surface showing protrusions the formation of stripe domains (sample bias −500 mV, tunnel current set point 55 pA). The (2×2) unit cell is indicated by green diamonds.

Note that due to the presence of modified ZrB_2 (0001) surface states, the silicene-diboride interface is metallic.[10,21] In general, for metallic materials, the latter two processes associated with the photoionization process as well as typically also the vibrational progressions lead to a (possibly structured) tail at the high-binding energy side.[22] Since the exact line shape is formed by a complex convolution of contributions from Gaussian (accounting for the experimental broadening), Lorentzian (due to life time effects) and Poisson-like (for vibrational degrees of freedom)[23,24] functions as well as due to an unknown tail from satellite features and possible other solid-state screening effects, we refrain for a more detailed discussion of the physics behind the line shape and in particular also of a discussion of the Gaussian/Lorentzian ratio that go beyond the statements made in this contribution.

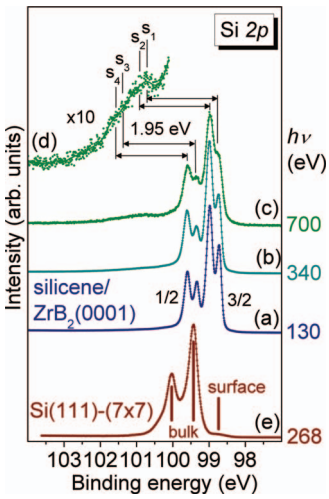

FIG. 2. (a)–(d) Normal-emission Si 2*p* photoelectron spectra of silicene on a thin ZrB_2(0001) film obtained at different photon energies: (a) $h\nu = 130$ eV, (b) $h\nu = 340$ eV, and (c) $h\nu = 700$ eV. (d) Magnification of the high-binding energy tail of the spectrum plotted as (d). Shake-up features s_1, s_2, s_3, and s_4 are identified 1.95 eV above the corresponding main peaks. (e) The normal-emission Si 2*p* spectrum of the Si(111)-(7 × 7) surface measured with $h\nu = 268$ eV.

In the present evaluation for $h\nu = 130$ eV, the asymmetry parameters are 0.05, 0.18, and 0.10 and the Gaussian/Lorentzian ratios are 0.70, 0.95, and 0.70, for the α, β, and γ components, respectively. Note that at the high-binding energy side, the full line representing the sum of the fitted individual components does not agree well with the experimental data points. This is likely due to an unresolved tail related to satellite features associated with the $2p_{3/2}$ peaks, as we will discuss later.

For the $2p_{3/2}$ line, the most intense component β is found at the binding energy of 98.98 ± 0.02 eV. Its $2p_{1/2}$ counterpart is shifted towards higher binding energy, the amount determined by the spin-orbit splitting of 600 ± 5 meV. Similar to the previous evaluation, the γ and α components are shifted 140 ± 3 meV and 260 ± 3 meV, respectively, towards lower binding energy with respect to β. Due to the higher experimental resolution, the full widths at half maximum of 140 meV, 180 meV, and 130 meV, for α, β, and γ, respectively, are significantly reduced as compared to the previous data.[10] The new spectrum reveals that the asymmetry parameter and the full width at half maximum are larger in particular for β which suggests that the associated peaks might derive from several chemical states which cannot be properly resolved by the fitting procedure. Further evidence for this hypothesis will be discussed later.

In Figure 2, spectra of silicene obtained with (a) $h\nu = 130$ eV, (b) 340 eV, and (c) 700 eV are compared to (e) a bulk-sensitive Si 2*p* spectrum of the clean Si(111)-(7 × 7) surface, obtained with $h\nu = 268$ eV. The bulk $2p_{3/2}$ component as assigned in Refs. 15 and 16 appears at a binding energy of 99.43 ± 0.05 eV and is indicated by a vertical line in Fig. 2. Note that for the Si(111)-(7 × 7) surface, E_F has been discussed to be pinned by a dangling bond state such that the core level binding energies may not depend on the doping level of the wafer.[25] Strikingly, the β, γ, and α components of the $2p_{3/2}$ line of silicene are shifted by 450 ± 70 meV, 590 ± 70 meV, and 710 ± 70 meV towards lower binding energy, respectively. Since the Si(111)-(7 × 7) surface[26] and silicene on ZrB_2 films[19] have very similar work functions,[13] this binding energy difference, as measured with respect to E_F, translates into similarly different core-level ionization energies as well. Note that equally large shifts towards lower binding energy have been observed for a number of reconstructed Si single crystal surfaces and attributed to the presence of Si surface atoms with dangling bonds: for the Si(111)-(7 × 7) surface the shift amounts to about 700 meV[16,18] (see the surface component marked as "surface" in Fig. 2(e)) and for the Si(100)-(2 × 1) and Si(100)-c(4 × 2) surfaces the shift for the topmost Si atom is about 450–550 meV.[16,18,27]

The observed binding energy difference is reminiscent of the one observed between the C 1*s* electrons of diamond and graphene. Note that the C 1*s* binding energy of sp^3-hybridized carbon atoms in the bulk of diamond (∼285.0 eV[28]) is about 0.8 eV higher than that of sp^2-hybridized atoms in graphene (∼284.2 eV[29]). This suggests that the low Si 2*p* binding energy is related to a certain degree of sp^2 hybridization for all of the Si atoms within the buckled honeycomb lattice of epitaxial silicene. It can then be understood that the binding energy positions of the α, β, and γ components are primarily caused by the buckling of the silicene layer characterized by a varying sp^2/sp^3 ratio, and only to a minor extent by the screening from and electronic coupling to the substrate which, as discussed previously, enhances the splitting among the individual components.[10]

B. Core-level satellite features

For the spectra shown in Fig. 2, obtained with $h\nu = 130$, 340, and 700 eV, as expected, the lower experimental resolution at higher photon energies leads to a broadening of the spectral features. Most importantly, at the high-energy side of the spectrum, the tail is enhanced with increasing $h\nu$. As shown in Fig. 2(e), for $h\nu = 700$ eV, the tail becomes even structured showing two groups of features that are split by 0.6–0.7 eV. Note that within the uncertainty of the evaluation, the splitting follows the value expected from the spin-orbit coupling. Since dynamical processes depend strongly on the excitation energy,[30,31] these satellite features may be related to either shake-up or plasmon excitations associated with the $2p_{3/2}$ and $2p_{1/2}$ main lines, respectively. These satellites, denoted as s_1, s_2, s_3, and s_4, are located at 1.95 ± 0.10 eV deeper than the four main peaks. This energy is close to the prominent peak at 1.7 eV in the calculated optical absorbance that is related to the predicted high optical transition strength between π bands at the *M* point of non-reconstructed, free-standing silicene.[32] The associated maximum in the joint density of states may lead to both shake-ups and the π plasmon resonance.

Provided that the silicene-derived partial density of states of the hybrid silicene-diboride surface is different from that of free-standing silicene,[21] the agreement may be accidental. On the other hand, it is established for carbon π electronic systems like graphite, fullerenes and carbon nanotubes that the π

plasmon frequency related to the collective excitation of all of the π electrons is closely associated with the maximum in the joint density of states related to the size of the transfer integral between atomic p orbitals in sp^2-hybridized systems.[33,34] A similar association might apply for silicene π electronic materials as well.

C. The atomic ratio of individual Si sites

The individual components α, β, and γ have been assigned to the three chemically distinguishable atomic sites, labelled as A, B, and C, within the $(\sqrt{3} \times \sqrt{3})$ unit cell of epitaxial silicene that represents itself as a (2×2) reconstruction of the ZrB_2 (0001) surface.[10] From the corresponding in-plane structure model shown in Fig. 1(b), the A:B:C atomic ratio is 2:3:1. Note that this model so far neglects the presence of stripe domains that have been revealed in large-scale scanning tunnelling microscopy (STM) images[10] similar to the one shown in Fig. 1(c). In this image obtained at room temperature, bright spots correspond to protrusions that might be associated with C-site atoms located in positions on top of Zr atoms.[35]

Figure 3(a) shows a selection of *Si* 2*p* spectra obtained in the photon energy range between 120 eV and 220 eV. When normalizing the intensity of the Si 2*p* spectra to the intensity of the β component, as done in Fig. 3(a), strong oscillations with $h\nu$ of the second main peaks related to the α and γ components, centered at binding energies of 98.72 eV and 99.32 eV, are clearly recognized. These oscillations are reminiscent of variations observed in the intensity ratio of components related to surface and bulk atoms in Si(111)-(7 × 7) core level spectra, and are related to photoelectron diffraction effects.[36] Any conclusion with regard to atomic ratios derived from these three components in silicene based on spectra obtained with just a few photon energies must therefore contain a certain margin of error that, however, can be diminished by considering the intensities of the three components in a wider energy range.

For the evaluation of the spectral intensities of the α, β, and γ components as a function of $h\nu$, the $2p_{3/2}$ line as normalized to the photon flux has been fitted in the energy range between 98.2 and 99.1 eV using asymmetric Poisson functions as discussed in Sec. III A. Fitting of the line at lower energies, e.g., the $2p_{3/2}$ line, alone using a cut-off energy largely avoids the uncertainty related to the high-energy tail from the $2p_{1/2}$ line that is superimposed to the $2p_{3/2}$ line. Note that given the restraints imposed by the chosen fitting functions, the fitting procedure is quite precise and robust. This is due to the quite perfect separation between the intense α and β peaks that allows for a good fit of the low- and high-energy flanks of the two main peaks, respectively. As expected, with increasing $h\nu$, the Gaussian width increases due to the lower experimental resolution while the Lorentzian width, the asymmetry ratio as well as the energy positions remain essentially unchanged. The results of the evaluation are shown in Fig. 3(b).

All of the three components show strong but different oscillations that are in particular strong at energies below 175 eV. In the inset of Fig. 3(b) are shown the intensities of

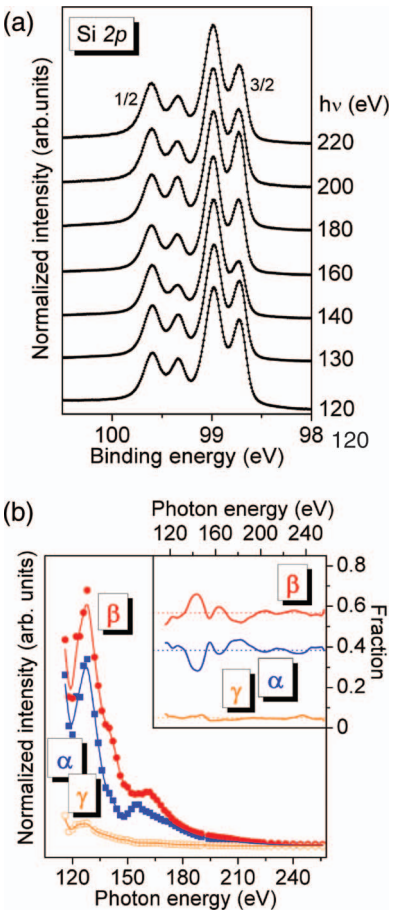

FIG. 3. (a) Normal-emission Si 2*p* spectra obtained in the photon energy range between 120 eV and 220 eV. The intensity of the Si 2*p* spectra is normalized to with respect to that of the β component. (b) Spectral intensities of the α (■), β (●), and γ (○) components as a function of the photon energy, as normalized to the photon flux. The inset shows the relative intensities of the α, β, and γ components as normalized to the total Si 2*p* intensity. Averaged intensities are shown by dotted lines.

the individual components as normalized to the total Si 2*p* intensity. Using this procedure, the intensities become independent from the energy-dependent transmission of the spectrometer and from the Si 2*p* atomic photoelectron emission cross-section. The average normalized intensities are found to oscillate around constant values shown as dotted lines. Using these average values, the corresponding ratio between α, β, and γ components is derived to be 2.3:3.4:0.3. Note that this ratio represents a substantial deviation from the model atomic ratio of 2:3:1. In particular, the γ component seems to be strongly underrepresented. Since A- and C-site atoms belong to the same sub-lattice and are chemically quite similar, it is possible that the α and γ components are not be properly identified by our peak fitting procedure. But even so, more than a third of the C-site atoms must be in a chemical environment δ that leads to a chemical shift close to that of β. This explanation is also consistent with the larger full width at half maximum of the β component, as discussed above.

Since the ratio does not follow the one expected from the model proposed to describe the $(\sqrt{3} \times \sqrt{3})$ unit cell of epitaxial silicene that relates itself to the (2×2) reconstruction of the ZrB_2(0001) surface, it is strongly suggested that the

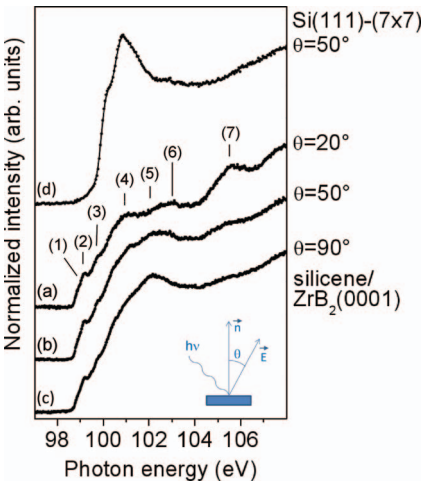

FIG. 4. Si 2*p* near-edge x-ray absorption fine structure spectra of silicene on a thin $ZrB_2(0001)$ film at (a) $\theta = 20°$, (b) 50°, and (c) 90°. Vertical bars indicate spectral features (1)–(6). (d) The corresponding spectrum of the Si(111)-(7 × 7) surface at $\theta = 50°$ is shown for comparison.

varying chemical state of C-site atoms is intrinsically linked to local structural deviations and thus to the formation of the stripe domains. Additionally, note that B-site atoms are located in between on-top and bridge positions.[10] Since on-top positions are the energetically least favourable ones,[14] shifting C-site atoms away from on-top positions may lower the total energy of the adsorbed silicene sheet. This, on the other hand, supports the hypothesis that the δ chemical state could relate to local structural deviations from the $(\sqrt{3} \times \sqrt{3})$ pattern. As such, considering the extent of domain boundaries visible in the STM image in Fig. 1(c), it may be conceived that C-site atoms in the δ chemical state are located within an extended boundary region while those in the γ chemical state are within the central parts of the stripes.

D. Angle-dependent NEXAFS spectra

In Figure 4 are shown Si 2*p* NEXAFS spectra of epitaxial silicene for the three angles $\theta = 20°$, 50° and 90°, with θ being defined as the angle between the electric field vector of the light and the normal of the sample. For comparison, the corresponding spectrum of the Si(111)-(7 × 7) surface at $\theta = 50°$ is shown.

The NEXAFS spectrum of silicene has a sharp onset at 98.7 eV that is followed by a steady increase until about 102.2 eV. Several resonances, denoted as (1) - (7), can be recognized as either shoulders or peaks. Features (1) - (4) do not show a dependence on θ while feature (5) increases and features (6) and (7) decrease with θ. Note that the relative transition strength related to both π^* and σ^* resonances depends on the orbital character (e.g., 2*p* or 1*s*) of the core electrons involved in the transitions which one should bear in mind when comparing the angular dependence of NEXAFS spectra of for instance graphite[37] or graphene[38] with those of silicene, obtained at different thresholds. While p-p transitions are dipole forbidden,[39] a transition from an orbital with p symmetry into π^* electronic states will occur with a minor intensity since π^* orbitals have a partial s character.[40] Additionally, for transitions from core orbitals with p symmetry into valence s orbitals, a vanishing angular dependence is expected.[39,40] Since features (1)–(4) do not exhibit any angular dependence, they may correspondingly be assigned to π^* resonances. For silicene on $ZrB_2(0001)$, unoccupied electronic states as close as 0.1 eV above E_F have been observed by scanning tunnelling spectroscopy[35] and by ARPES as a state shifted below E_F following the adsorption of K atoms.[13] The appearance of π^* resonances in the NEXAFS spectrum would then be highly consistent with the assignment of a π^* character to these states.

In this context, it is important to compare the spectrum to that obtained from surfaces of Si wafers.[16,41] In the spectrum of the Si(111)-(7 × 7) surface shown in Fig. 4(d), the steep onset of bulk-related absorption at about 99.6 eV[41] has σ^* character, while a pre-resonance with a minor spectral weight at about 98.6 eV, more clearly visible in the surface-sensitive mode for the Si(100)-(2 × 1) surface,[16] may possibly be attributed to the top-most Si atoms. These atoms are thought to be in a sp^2 bonding configuration.[27] The comparison shows that it is reasonable to assign the σ^* absorption onset in silicene to photon energies in between 99 and 99.5 eV, by taking into account the Si 2*p* binding energy difference between silicene and the bulk of sp^3-hybridized silicon. In contrast to the case of graphite[30] and graphene,[31] the energies of the onsets of π^* and σ^* absorption in silicene might not be so far from each other since the total band widths of π^* and σ^* bands are less than half of those in graphene.[1,2,13]

IV. CONCLUSIONS

In conclusion, high-resolution Si 2*p* photoelectron and NEXAFS spectra contain a wealth of information related to the structural and electronic properties of $(\sqrt{3} \times \sqrt{3})$-reconstructed and buckled epitaxial silicene. In particular, the core level binding energies are generally lower than those of sp^3-hybridized Si atoms in the bulk of silicon single crystals and reflect the varying sp^2/sp^3 ratio for the distinct atomic sites. The analysis of the intensity of individual components in a wide photon energy range is used to obtain the ratio of Si atoms at various sites, and reveals an abundance of C-site atoms that is significantly lower than expected from the proposed structure model. Since the C sites correspond to energetically unfavourable on-top positions, we propose that this is related to a relaxation of the silicene sheet such that these atoms adopt a different position within the extended boundary regions in between stripe domains observed in STM images. This is consistent with the relatively large full width at half maximum of the XPS features corresponding to B-site atoms, where the broadening could be due to the presence of atoms that have shifted away from the C sites.

While it is difficult to obtain optical reflectance spectra for silicene on $ZrB_2(0001)$ or Ag(111) surfaces, the appearance of photoelectron satellite features close to predicted peak energies in the optical absorbance suggests a relation with interband transitions between π bands at and in the vicinity of the *M* point of non-reconstructed silicene.

The Si 2*p* x-ray absorption onset is found to be below that of Si atoms in sp^3 bonding configurations and is caused

by transitions into states with π^* character. The study of core level excitations is therefore a powerful tool for the identification of epitaxial silicene and its remarkable structural and electronic properties. This capacity will be crucial for the characterization of low-dimensional Si nanostructures needed to create a future silicene-based electronics.

ACKNOWLEDGMENTS

We are grateful for experimental help from K. Mase (Institute of Materials Structure Science, High Energy Accelerator Research Organization, Tsukuba, Japan) and from A. B. Preobrajenski and J. Osiecki (MAX-Lab, Lund, Sweden). Y.Y.-T. acknowledges financial support from a Funding Program for Next-Generation World-Leading Researchers (GR046), and M.P.d.J., H.V.B., and F.B.W. by the research program of the Foundation for Fundamental Research on Matter (FOM, Grant No. 12PR3054), which is part of the Netherlands Organization for Scientific Research (NOW). This work has been performed under the approval of the Photon Factory (Proposal No. 2012G610) and MAX-Lab Advisory Committees (Proposal No. 20130141).

[1]K. Takeda and K. Shiraishi, Phys. Rev. B **50**, 14916 (1994).
[2]G. G. Guzmán-Verri and L. C. Lew Yan Voon, Phys. Rev. B **76**, 075131 (2007).
[3]C. C. Liu, W. Feng, and Y. Yao, Phys. Rev. Lett. **107**, 076802 (2011).
[4]M. Ezawa, Phys. Rev. Lett. **109**, 055502 (2012).
[5]M. Ezawa, New J. Phys. **14**, 033003 (2012).
[6]W.-F. Tsai, C.-Y. Huang, T.-R. Chang, H. Lin, H.-T. Jeng, and A. Bansil, Nat. Commun. **4**, 1500 (2013).
[7]C. L. Lin, R. Arafune, K. Kawahara, N. Tsukahara, E. Minamitami, Y. Kim, N. Takagi, and M. Kawai, Appl. Phys. Express **5**, 045802 (2012).
[8]H. Jamgotchian, Y. Colignon, N. Hamzaoui, B. Ealet, J. Y. Hoarau, B. Aufray, and J. P. Bibérian, J. Phys. Condens. Matter **24**, 172001 (2012).
[9]P. Vogt, P. De Padova, C. Quaresima, J. Avila, E. Frantzeskakis, M. C. Asensio, A. Resta, B. Ealet, and G. Le Lay, Phys. Rev. Lett. **108**, 155501 (2012).
[10]A. Fleurence, R. Friedlein, T. Ozaki, H. Kawai, Y. Wang, and Y. Yamada-Takamura, Phys. Rev. Lett. **108**, 245501 (2012).
[11]L. Meng, Y. Wang, L. Zhang, S. Du, R. Wu, L. Li, Y. Zhang, G. Li, H. Zhou, W. A. Hofer, and H.-G. Gao, Nano Lett. **13**, 685 (2013).
[12]C. L. Lin, R. Arafune, K. Kawahara, M. Kanno, N. Tsukahara, E. Minamitani, Y. Kim, M. Kawai, and N. Takagi, Phys. Rev. Lett. **110**, 076801 (2013).
[13]R. Friedlein, A. Fleurence, J. T. Sadowski, Y. Yamada-Takamura, Appl. Phys. Lett. **102**, 221603 (2013).
[14]C.-C. Lee, A. Fleurence, R. Friedlein, Y. Yamada-Takamura, and T. Ozaki, Phys. Rev. B **88**, 165404 (2013).
[15]T. Miller, T. C. Hsieh, and T.-C. Chiang, Phys. Rev. B **33**, 6983 (1986).
[16]F. J. Himpsel, P. Heimann, T.-C. Chiang, and D. E. Eastman, Phys. Rev. Lett. **45**, 1112 (1980).
[17]C. J. Karlsson, E. Landemark, L. S. O. Johansson, U. O. Karlsson, and R. I. G. Uhrberg, Phys. Rev. B **41**, 1521 (1990).
[18]J. Yoshinobu, Prog. Surf. Sci. **77**, 37 (2004).
[19]Y. Yamada-Takamura, F. Bussolotti, A. Fleurence, S. Bera, and R. Friedlein, Appl. Phys. Lett. **97**, 073109 (2010).
[20]J. D. Bozek, G. M. Bancroft, J. N. Cutler, and K. H. Tan, Phys. Rev. Lett. **65**, 2757 (1990).
[21]C.-C. Lee, A. Fleurence, Y. Yamada-Takamura, T. Ozaki, and R. Friedlein, "Band structure of silicene on the zirconium diboride (0001) thin film surface: Convergence of experiment and calculations in the one-Si-atom commensurate Brillouin zone" (unpublished).
[22]S. Doniach and M. Sunjic, J. Phys. C: Solid State Phys. **3**, 285 (1970).
[23]I. Minkov, F. Gel'mukhanov, R. Friedlein, W. Osikowicz, C. Suess, G. Öhrwall, S. L. Sorensen, S. Braun, R. Murdey, W. R. Salaneck, and H. Ågren, J. Chem. Phys. **121**, 5733 (2004).
[24]R. S. Sánchez-Carrera, V. Coropceanu, D. A. da Silva Filho, R. Friedlein, W. Osikowicz, R. Murdey, C. Suess, W. R. Salaneck, and J.-L. Brédas, J. Phys. Chem. B **110**, 18904 (2006).
[25]F. J. Himpsel, G. Hollinger, and R. A. Pollak, Phys. Rev. B **28**, 7014 (1983).
[26]K. Sakamoto, T. Okuda, H. Nishimoto, H. Daimon, S. Suga, T. Kinoshita, and A. Kakizaki, Phys. Rev. B **50**, 1725 (1994).
[27]E. Landemark, C. J. Karlsson, Y.-C. Chao, and R. I. G. Uhrberg, Phys. Rev. Lett. **69**, 1588 (1992).
[28]J. F. Morar, F. J. Himpsel, G. Hollinger, J. L. Jordan, G. Hughes, and F. R. McFeely, Phys. Rev. B **33**, 1340 (1986).
[29]S. Lizzit, G. Zampieri, L. Petaccia, R. Larciprete, P. Lacovig, E. D. L. Rienks, G. Bihlayer, A. Baraldi, and P. Hofmann, Nat. Phys. **6**, 345 (2010).
[30]J. Stöhr, R. Jaeger, and J. J. Rehr, Phys. Rev. Lett. **51**, 821 (1983).
[31]N. Wassdahl, J.-E. Rubensson, G. Bray, P. Glans, P. Bleckert, R. Nyholm, S. Cramm, N. Mårtensson, and J. Nordgren, Phys. Rev. Lett. **64**, 2807 (1990).
[32]F. Bechstedt, L. Matthes, P. Gori, and O. Pulci, Appl. Phys. Lett. **100**, 261906 (2012).
[33]J. Fink, Adv. Electron. Electron Phys. **75**, 121 (1989).
[34]T. Pichler, M. Knupfer, M. S. Golden, J. Fink, A. Rinzler, and R. Smalley, Phys. Rev. Lett. **80**, 4729 (1998).
[35]A. Fleurence, Y. Yoshida, C.-C. Lee, Y. Yamada-Takamura, and Y. Hasegawa, Appl. Phys. Lett. **104**, 021605 (2014).
[36]J. A. Carlisle, M. T. Sieger, T. Miller, and T.-C. Chiang, Phys. Rev. Lett. **71**, 2955 (1993).
[37]R. A. Rosenberg, P. J. Love, and V. Rehn, Phys. Rev. B **33**, 4034 (1986).
[38]D. Pacilé, M. Papagno, A. Fraile Rodríguez, M. Grioni, L. Papagno, Phys. Rev. Lett. **101**, 066806 (2008).
[39]I. Tanaka and H. Adachi, J. Phys. D: Appl. Phys. **29**, 1725 (1996).
[40]Y. Ma, P. Rudolf, C. T. Chen, and F. Sette, J. Vac. Technol. A **10**, 1965 (1992).
[41]F. C. Brown, R. Z. Bachrach, and M. Skibowski, Phys. Rev. B **15**, 4781 (1977).